Materials Science Forum
ISSN: 1662-9752, Vol. 1180, pp 69-75
doi:10.4028/p-O3Bp7s

Submitted: 2025-05-27
Revised: 2025-12-05
Accepted: 2025-12-19
Online: 2026-03-04

Roman Bronze Objects from the Archaeological Site of Burg in Burgenland, Austria

Susanne Strobl[1,a] and Roland Haubner[1,b*]

[1]Technische Universität Wien, Institute of Chemical Technologies and Analytics, Getreidemarkt 9/164-03, A-1060 Vienna, Austria

[a]susanne.strobl@tuwien.ac.at, [b*]roland.haubner@tuwien.ac.at

Keywords: bronze, small parts, roman, microstructures.

Abstract. Several Roman bronze objects were confiscated from a digger, which had been collected illegally at the archaeological site of Burg, Burgenland. Since these parts are archaeologically worthless, they were allowed to be examined with destructive analysis methods. The investigative results of five parts are presented. The surface of the parts is covered with a green patina which contains mainly Cu and smaller amounts of Sn, Pb, P, Ca, Al, S and Fe. If XRF analyses are performed, it must be taken into account that elements such as Sn accumulate in the patina. The average XRF analyses of the hook showed a content of 0.8 wt.% Sn and about 2 wt.% Pb, but in the fibular parts and the button up to 42 wt.% Pb were detected. Due to very different compositions of the samples, the microstructures are also appropriate miscellaneous. It is possible to distinguish between cast, recrystallized and deformed microstructures. These investigations show that the Roman metallurgist used a wide variety of copper alloys, because raw and recycled materials were probably processed together.

Introduction

It is usually difficult to obtain historical objects for examination using destructive testing methods, as such objects possess cultural value and must be preserved. Exceptions exist, e.g. when objects are on hand in large numbers [1–4] or their origin is not clearly established [5–7].

In this work the investigated samples were confiscated from a metal detectorist and were available for examination. The objects have been classified by an archaeologist as Roman and it was reported that they come from the Burg archaeological site in Burgenland, Austria [8].

So far, we had the possibility to examine by metallography a Roman bronze fibula [6], a bronze tip – the producer is uncertain [7], probably Roman provenance - and several objects made of copper or copper alloys from the Bronze Age [9–11].

For bronze objects, it seems to be necessary to produce several metallographic sections, because inhomogeneities can occur due to the bronze casting process, which can pervert the results of localized sampling [12]. Furthermore, analysis should not be performed solely on the surface, as corrosion leads to an accumulation of Sn in the corrosion products and you get no information about the bulk microstructure [13].

Experimental Procedure

First the objects were photographed and subsequently cold mounted in epoxy resin under vacuum. Once hardened, the metallographic preparation was carried out in stages by grinding and polishing up to a diamond grain size of 1 µm. The sections were analyzed in the as-polished state and after etching with Klemm 2 or $(NH_4)_2CuCl_4$ solution.

A light optical microscope (LOM) and a scanning electron microscope (SEM) with Electron Backscattering Detector (BSE) and with energy dispersive X-ray analysis (EDX) were used. To determine the overall chemical composition of the samples, measurements were additionally carried out on the metallographic sections using X-ray fluorescence analyses (XRF).

Results and Discussion

XRF measurements.

The XRF analyses performed on the metallographic sections are summarized in Table 1. It should also be noted that minor errors may occur, because the corrosion layer is partially included. In these measurements it is already noticeable that the Pb contents are high (up to 42 wt.%) and fluctuate extremely (minimum: 2 wt.%). The contents of Sn and Zn also vary remarkably.

Table 1. XRF results of the bronzes (wt.%) measured at the metallographical cross sections.

Element	Burg 1	Burg 2	Burg 3	Burg 4	Burg 5
Cu	96.4	56.66	69.65	56.82	48.87
Sn	0.79	12.86	3.73	8.71	6.5
Pb	1.92	26.82	22.88	30.07	41.78
Sb	0.4	0.87	0.09	0.7	0.2
Zn	n.n.	1.93	1.42	3.33	1.62
S	n.n.	0.12	1.55	n.n.	0.06
P	0.09	0.3	0.07	n.n.	0.16
Si	0.13	0.2	0.11	n.n.	0.31
Fe	0.27	0.24	0.27	0.38	0.42
Al	n.n.	n.n.	0.05	n.n.	0.08

A copper hook (Burg 1).

According to XRF measurements (Table 1), the hook examined consists predominantly of copper with approximately 0.8 wt.% Sn and 2 wt.% Pb.

Corrosion products with Sn enrichments are visible on the surface (Fig. 1a–c), which were detected by EDX. Elevated concentrations of P (up to 5 wt.%) and Ag (up to 0.9 wt.%) were locally measured. Also, boron was detected at some locations, but a quantification with EDX measurements is impossible. May be the elements Ag, B, and P reached the surface due to a soldering process, but this is not certain.

The cross-section shows that the bent part of the hook is significantly thicker than the straight part (Fig. 1d). This indicates that the hook was manufactured by forging and is additionally confirmed by the microstructure. In the undeformed part the grain size is up to 100 µm (Fig. 1e). In the deformed part the grain size is significantly smaller with up to 20 µm (Fig. 1f), but elongated inclusions of lead are visible (Fig. 1f–h). The corrosion layer can be seen on the surface (Fig. 1i).

A fibula pin catch (Burg 2).

The XRF measurements show that the fibula pin catch is made of bronze with 13 wt.% Sn and 27 wt.% Pb (Table 1) (Fig. 2a). These values could be somewhat too high, if the proportion of corrosion products was measured simultaneously.

In the as-polished condition dark Pb and gray corrosion products can be identified (Fig. 2b, c) and after etching a dendritic microstructure is observed (Fig. 2d–f), indicating a production by casting.

Small and bright precipitates of the intermetallic phase $Cu_{41}Sn_{11}$ are visible additionally (Fig. 2e). Polarized light clearly shows different orientated dendritic regions formed during solidification, as well as the corrosion product malachite, which appears green (Fig. 2f).

A fibula head (Burg 3).

According to XRF measurements the fibula head contains 4 wt.% Sn and 23 wt.% Pb (Table 1) (Fig. 3a). The Sn content is somewhat low for a bronze.

A cross-section through the head appears rather homogeneous with large black spots, which were identified as Pb inclusions (Fig. 3b). A closer look reveals the presence of large and small Pb aggregates (Fig. 3c, f, g). The large aggregates are usually oval with a size up to 300 µm. The small ones are irregularly shaped in the range of 10 µm (Fig. 3g). It is assumed that this distribution of Pb is a result of the high Pb content and segregation effects during solidification of the melt.

The Cu-Pb phase diagram is unique, because it exhibits a monotectic behavior in the concentration range between 37.4 and 86 wt.% Pb in Cu [14]. This means that two melts of different compositions exist side by side. The ternary Cu-Pb-Sn phase diagram is somewhat more complex: the addition of Sn increases the region containing two melts and simultaneously reduces the temperature range of solidification [15]. The linear arrangement of Pb aggregates (Fig. 3d) can be explained by the fact, that the melt solidifies from the rim to the core resulting in an enrichment of alloying elements at the solidification front. Copper exhibits a dendritic solidification structure (Fig. 3e), and an additional bright phase is visible, which can be interpreted as Cu-Sn phase (Fig. 3h). The large, partially Pb-filled, oval inhomogeneity could be a mixture of shrinkage cavity and Pb precipitation (Fig. 3g).

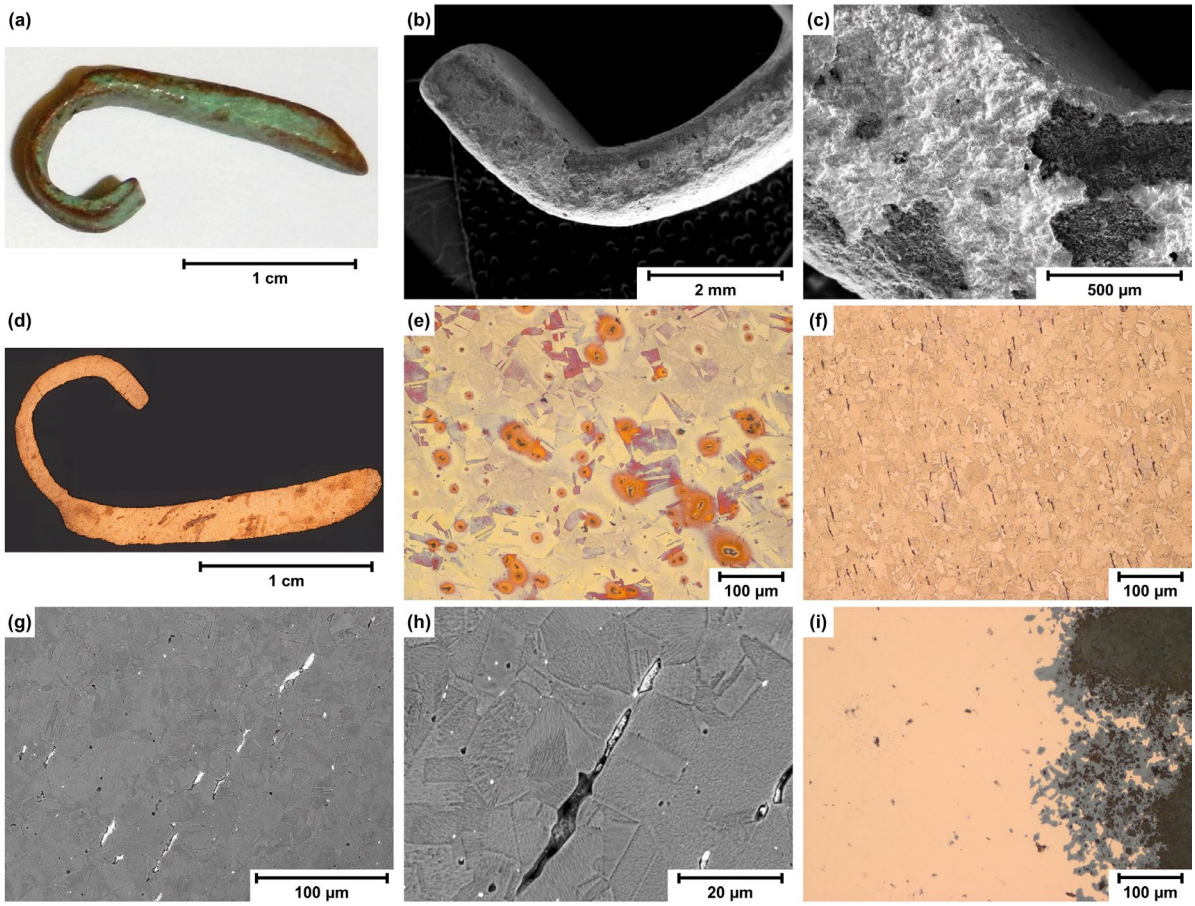

Fig. 1. Copper hook (Burg 1). (a) photo, (b, c) surface, SEM (d–f) cross section, LOM, (d–f) $(NH_4)_2CuCl_4$ etched, (g, h) SEM, (i) polished, LOM.

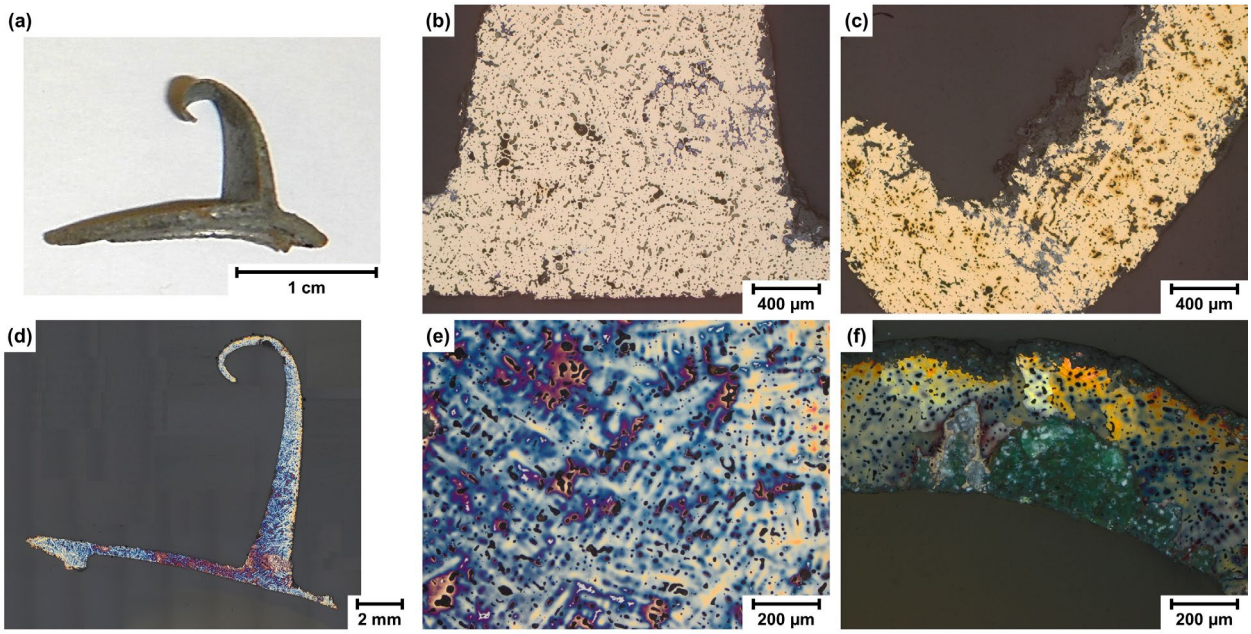

Fig. 2. Fibula pin catch (Burg 2). (a) photo, (b, c) polished, LOM, (d, e) Klemm 2 etched, LOM (f) polarized light, LOM.

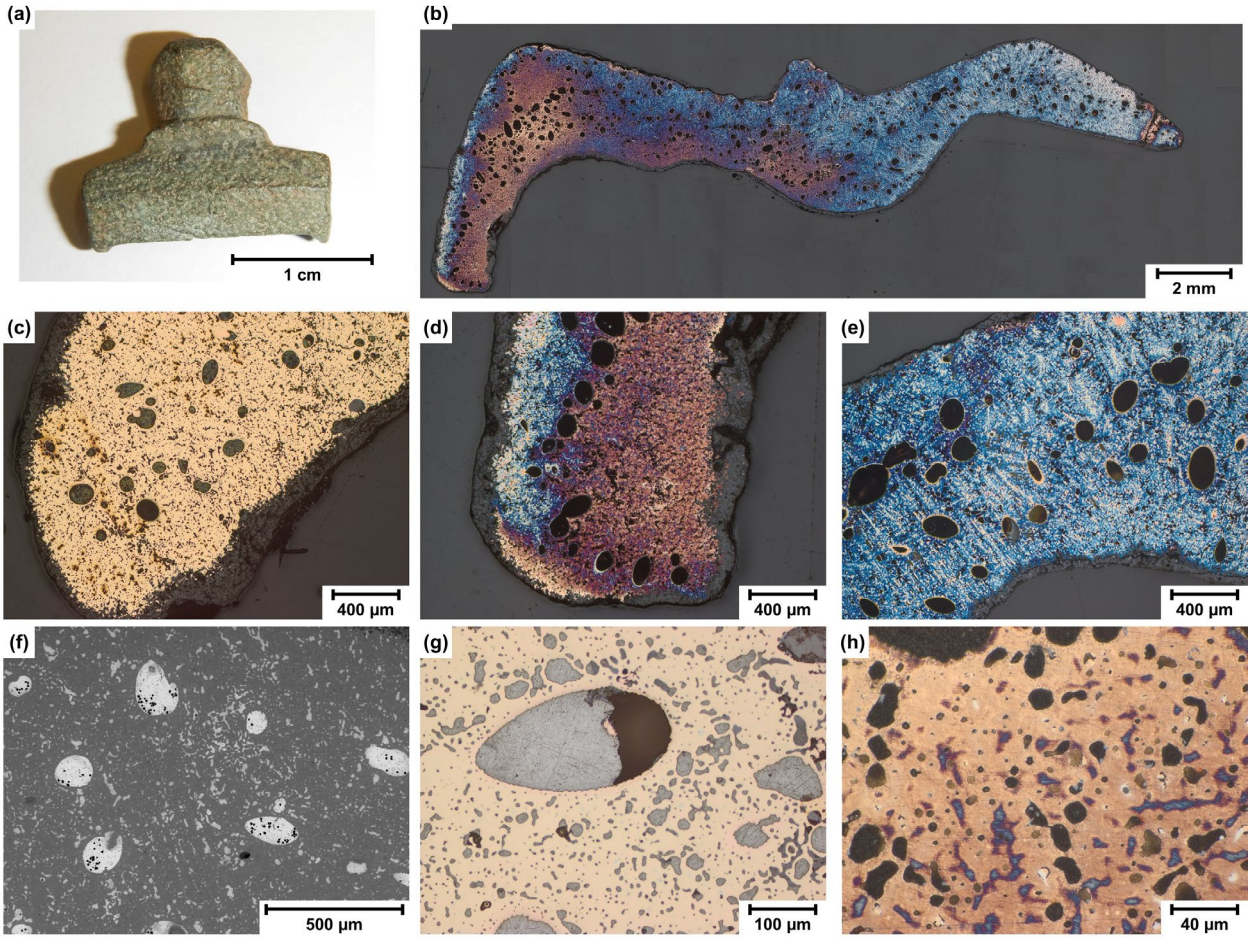

Fig. 3. Fibula head (Burg 3). (a) photo, (b) cross section, Klemm 2 etched, LOM, (c, g) polished LOM, (d, h) Klemm 2 etched, (f) SEM.

A fibula food (Burg 4).

The fibula food contains 9 wt.% Sn and 30 wt.% Pb, more of both elements than the previously described fibula head. It contains additionally 3 wt.% Zn (Table 1) (Fig. 4a).

As expected from the XRF analysis, this alloy contains numerous precipitates of Pb and a Cu-Sn phase (Fig. 4d, f). Also the dendritic solidification of copper is clearly visible (Fig. 4c, f), but large Pb inclusions - seen in the fibula head - are not visible.

The hook shown in Fig. 4b is the catch of the fibula foot. Increased corrosion is visible inside (Fig. 4b, e) and a distinct corrosion layer is also visible outside (Fig. 4f). The enrichment of Pb and Sn in the corrosion products may have led to relative high XRF values.

A bronze button (Burg 5).

The investigated button has a central pin and no eyelet (Fig. 5a). The pin and the extraordinary high Pb content (42 wt.% Pb, 6.5 wt.% Sn) distinguishes it from previously examined buttons from the Iron and Bronze Ages (Table 1) [16, 17].

The microstructure is homogeneous over the cross-section (Fig. 5b). The microstructure shows a dendritic solidification (Fig. 5c–e) of copper and numerous precipitations in the interdendritic areas (Fig. 5f–h). Although the Pb content measured by XRF is approximately twice that of the fibula head, the Pb inclusions are relatively small with a size up to 40 µm.

These results indicate that the button underwent no further heat treatment after its casting.

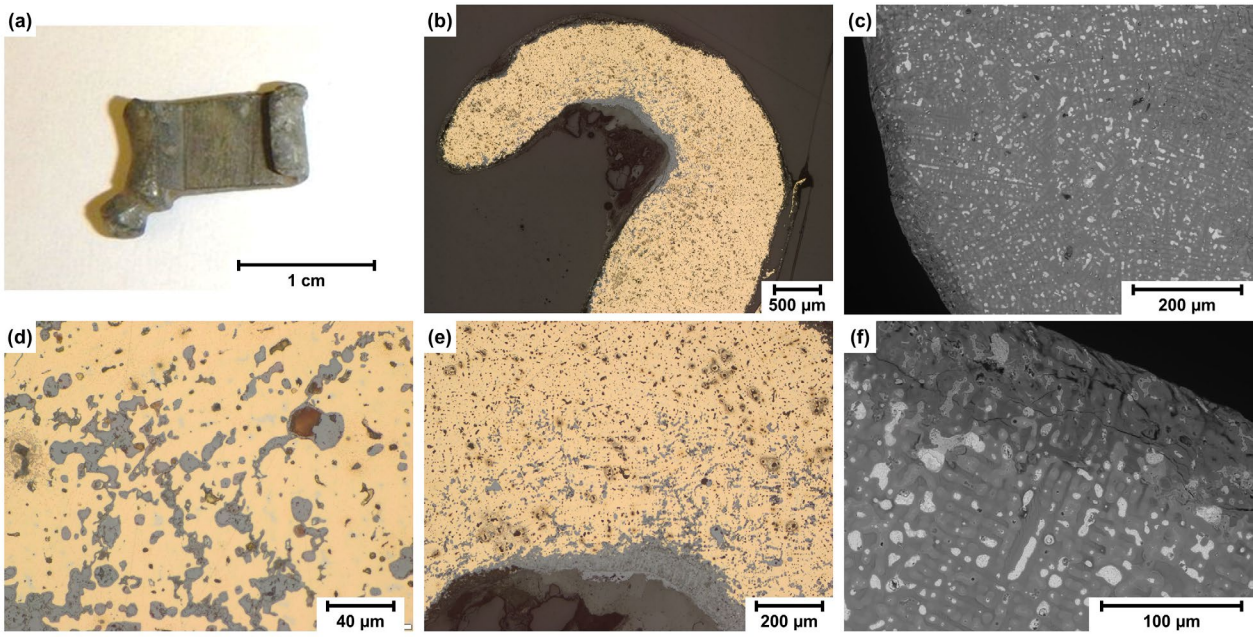

Fig. 4. Fibula food (Burg 4). (a) photo, (b, d, c) polished, LOM, (c, f) SEM.

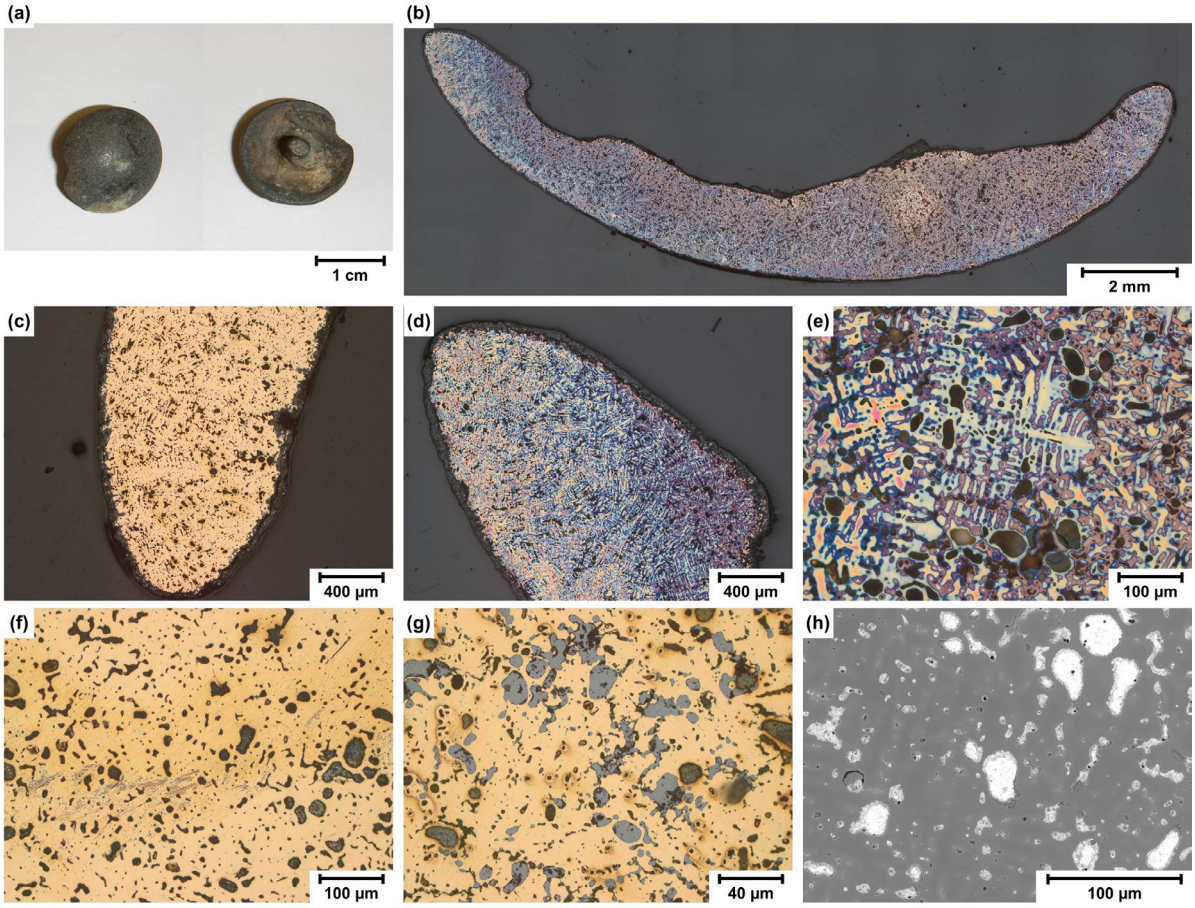

Fig. 5. Bronze button (Burg 5). (a) photos avers and revers, (b) overview, (b, d, e) Klemm 2 etched, LOM, (c, f, g) polished, LOM, (h) SEM.

Summary

A prerequisite for these investigations was that the objects could be destroyed to carry out metallographic examinations. The analyzed samples were a bronze hook, a fibula pin catch, a fibula head, a fibula food and a bronze button.

The examined hook consists of copper with small amounts of Pb and Sn. Its microstructure is recrystallized and deformed.

The fibula parts and the button are quite different from the hook, because all of them contain more than 23 wt.% Pb. The button had the highest Pb content with 42 wt.% Pb.

Since the other components of the bronze influence the microstructures, there are some differences among the examined samples. However, it is suspected that at high concentrations of Pb and Sn, large Pb aggregates can be formed due to the melting behavior of the alloy.

The patina of all parts is green, but it should be noted that in particular Sn and Pb can be concentrated in the corrosion products. This can lead to misinterpretation of the measurement results.

Regardless of the alloy composition, it is possible to distinguish between cast, recrystallized and deformed microstructures.

These investigations show that the Roman metallurgist used a wide variety of copper alloys, because raw and recycled materials were probably processed together.

Acknowledgement

The authors would like to thank the TU Wien Library for the financial support through its Open Access Funding Program.

References

[1] R. Haubner, S. Strobl, Materials Science Forum, 782 (2014) 635-640.

[2] R. Haubner, S. Strobl, Pract. Metallogr., 59 (2022) 720-731.

[3] W. Scheiblechner, S. Karl, D. Modl, S. Strobl, R. Haubner, BHM Berg- und Hüttenmännische Monatshefte, 166 (2021) 363-369.

[4] R. Haubner, S. Strobl, J. Leskovar, Pract. Metallogr., 61, 9-10 (2024) 630-641.

[5] R. Haubner, F. Ertl, S. Strobl, Pract. Metallogr., 54 (2017) 107-117.

[6] R. Haubner, A. Pronina, S. Strobl, Metallography, Microstructure, and Analysis, 14 (2025) 652-662.

[7] R. Haubner, S. Strobl, BHM Berg- und Hüttenmännische Monatshefte, 169, 9 (2024) 483-489.

[8] W. Meyer, Burgenländische Heimatblätter, 46 (1984) 145-167.

[9] R. Haubner, S. Strobl, Metallography, Microstructure, and Analysis, 12 (2023) 187–201.

[10] R. Haubner, S. Strobl, M. Thurner, H. Herdits, BHM Berg- und Hüttenmännische Monatshefte, 166 (2021) 352-357.

[11] R. Haubner, S. Strobl, Pract. Metallogr., 59 (2022) 749-760.

[12] R. Haubner, S. Strobl, Pract. Metallogr., 59 (2022) 732-748.

[13] R. Haubner, S. Strobl, P. Trebsche, Materials Science Forum, 891 (2017) 41-48.

[14] T.B. Massalski, Binary Alloy Phase Diagrams. ASM International, Metals Park OH (1990).

[15] R. Cayumil, R. Khanna, M. Ikram-Ul-Haq, R. Rajarao, A. Hill, V. Sahajwalla, Waste Management, 34 (2014) 1783-1792.

[16] R. Haubner, Pract. Metallogr., 60 (2023) 276-288.

[17] R. Haubner, S. Strobl, J. Leskovar, Metallography, Microstructure, and Analysis, 13 (2024) 1119-1130.

The publication of this article was funded by the TU Wien 10.13039/501100004729